Author(s): Tynjälä, Pekka; Laine, Petteri; Välikangas, Juho; Kauppinen, Toni; Lassi, Ulla

Title: Effect of Reaction Conditions on the Coprecipitation of Ni(OH)2 for Lithium-Ion Batteries

Year: 2023

Version: Published version

Please cite the original version:

Tynjälä, P., Laine, P., Välikangas, J., Kauppinen, T., & Lassi, U. (2023). Effect of Reaction Conditions on the Coprecipitation of Ni(OH)2 for Lithium-Ion Batteries. Chemical Engineering and Technology, 46(11), 2279-2284. https://doi.org/10.1002/ceat.202300086

Pekka Tynjälä[1,2,*]
Petteri Laine[1,2]
Juho Välikangas[1,2]
Toni Kauppinen[1,2]
Ulla Lassi[1,2]

Effect of Reaction Conditions on the Coprecipitation of $Ni(OH)_2$ for Lithium-Ion Batteries

Electrochemical performance of cathode active materials (CAMs) is dependent on the properties of coprecipitated precursors (pCAMs). This is a sensitive process affected by several reaction parameters such as temperature, pH, concentration of reactants, agitation rate, and residence time. In this paper, the effect of parameters influencing the particle size growth and the physical properties, such as particle morphology and tapped density, was studied in the coprecipitation of $Ni(OH)_2$. Formation of a homogeneous population with narrow particle size distribution was observed, followed by a more heterogeneous population of dense particles. Ammonia concentration and residence time had significant effects on particle size growth and morphology, but agitation rate also had an impact.

Keywords: Battery chemicals, Coprecipitation of $Ni(OH)_2$, Lithium-ion batteries, Nickel hydroxide

Received: February 05, 2023; *revised:* March 25, 2023; *accepted:* May 25, 2023

DOI: 10.1002/ceat.202300086

1 Introduction

Lithium-ion batteries (LIBs) are extensively used in portable electronics and electric vehicle (EV) applications due to their high energy, power density, and enhanced cycle life compared to other rechargeable batteries, such as lead-acid or NiMH batteries [1]. Pure $LiNiO_2$ (LNO) is a promising candidate as a cathode material in Li-ion batteries, as it is Co-free and has a high theoretical capacity of 274 mAh g^{-1} [2–5]. The electrochemical properties of cathode materials may be taylored during the coprecipitation of precursors by applying procedures such as, e.g., doping with varying elements [6] and by coprecipitation of precursors having concentration gradients of transition metals within the secondary particles [7].

Key LNO properties are tailored prior to lithiation during the coprecipitation of precursor $Ni(OH)_2$ [4]. In addition to its chemical composition, these include tapped density (porosity), particle size, and secondary particle size distribution. These morphological features of the active particles are usually determined during the synthesis of $Ni(OH)_2$ [8].

Several possibilities are available for making LNO, such as coprecipitation, sol-gel synthesis [9], and solid-state reactions at high temperature [10]. Coprecipitation is the industrially relevant method and is considered in this paper. During the coprecipitation, several parameters are present simultaneously, affecting the particle size growth and particle morphology [11]. The optimization of precipitation parameters may be challenging and time-consuming because some parameters may influence another. For example, changing the pH may alter the concentration of ammonia and thus affecting the concentration of transition metal ammine complexes [12]. Also, the change of agitation rate may alter the effective volume of a reactor, thus affecting the residence time of the process. Therefore, optimized coprecipitation conditions may be considered as a compromise for several parameters applied for a certain reactor configuration.

In this paper, the effect of reaction conditions on the coprecipitation of nickel hydroxide cathode precursor material was studied. In the series of coprecipitation experiments, the impact of process variables, such as reactant concentration, ammonia concentration, residence time, and agitation rate, was studied.

2 Experimental

2.1 Coprecipitation of $Ni(OH)_2$

Spherical $Ni(OH)_2$ precursors were synthetized using alkali metal hydroxide (NaOH) coprecipitation in an inert gas (nitrogen) atmosphere, according to literature references [13, 14]. Inert gas was used to prevent the oxidation of precursor. Pre-

[1]Dr. Pekka Tynjälä (pekka.tynjala@oulu.fi), Petteri Laine, Juho Välikangas, Toni Kauppinen, Prof. Ulla Lassi
https://orcid.org/0000-0001-5319-9525
University of Oulu, Research unit of Sustainable Chemistry, Pentti Kaiteran katu 1, 90570 Oulu, Finland.
[2]Dr. Pekka Tynjälä, Petteri Laine, Juho Välikangas, Toni Kauppinen, Prof. Ulla Lassi
University of Jyvaskyla, Kokkola University Consortium Chydenius, Talonpojankatu 2 B, 67100 Kokkola, Finland.

cipitation was conducted in a continuous-flow stirred-tank reactor (CSTR) with a reactor volume of 3 L at temperatures of 40, 50, or 60 °C under vigorous agitation (Fig. 1) using different agitation rates. The key parameters during the coprecipitation included temperature, pH, agitation rate, residence time, as well as hydroxide, ammonia, and metal solution concentrations.

Figure 1. Continuous stirred-tank reactor used for coprecipitation.

The reactor was preloaded with deionized water; then, aqueous solutions of metal sulfate $NiSO_4 \cdot 6H_2O$, NaOH, and concentrated ammonia were fed separately to the reactor using peristaltic pumps. The ammonia concentration in the solution was measured frequently during the precipitation and it was adjusted based on the target ammonia concentration during the experiment.

Particle size growth during $Ni(OH)_2$ coprecipitation was followed by determining the particle size distribution of the slurry sampled from the reactor's overflow tubing. The solution was heated to a precipitation temperature, and the pH was adjusted to a desired level with NaOH solution. The feeding rates of nickel sulfate, NaOH, and ammonia solutions were adjusted to maintain the desired residence time. After coprecipitation, the precursor slurry was filtered in a vacuum, and the precipitate was carefully washed with a sufficient amount of warm deionized water. The synthetized $Ni(OH)_2$ precursors were dried overnight at 60 °C in a vacuum oven.

2.2 Characterization of $Ni(OH)_2$

The tapped density was measured using an Erweka SVM 222 tapped density analyzer according to the ISO EN 787/11 standard. The evolution of particle size distribution during coprecipitation was followed using a Malvern Mastersizer 3000. The ammonia concentration of the mother liquor was analyzed by automatic titration using a 1 mol L^{-1} HCl solution. Field emission scanning electron microscopy (FESEM) images of the particle microstructure were obtained on a Zeiss Sigma at the Centre for Material Analysis of the University of Oulu, operating at 5 kV.

3 Results and Discussion

3.1 Effect of Temperature on Precipitation

Coprecipitation is typically done at temperatures of 40–80 °C. The temperature is known to have a significant effect on coprecipitation kinetics of transition metal hydroxide materials [15]. In this study, the impact of precipitation temperature was first studied using temperatures of 40–60 °C. The morphology of the precipitated $Ni(OH)_2$ particles was followed and is presented in Fig. 2.

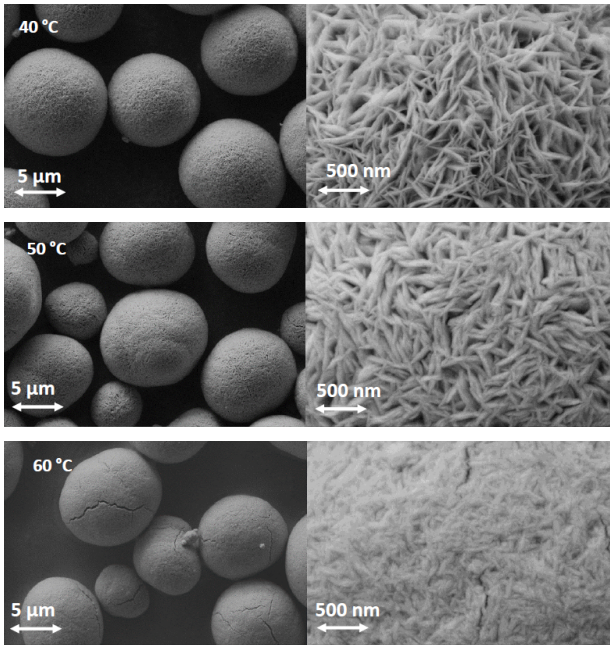

Figure 2. Effect of precipitation temperature on the morphology of precursors.

According to FESEM imaging, the higher precipitation temperature led to the formation of more closely packed primary particles. At the highest precipitation temperature, cracking of the secondary particles was observed. The obtained particle morphology presented in Fig. 2 is comparable to that reported earlier by Yang et al. [11]. The determined tapped density values for the precursors precipitated at different temperatures are given in Tab. 1. They were consistent with visual observations.

Table 1. Tapped density values for the $Ni(OH)_2$ precursors precipitated at different temperatures.

Precipitation temperature [°C]	Tapped density [g cm^{-3}]
40	1.86
50	2.00
60	2.07

The most homogeneous particle size distribution with acceptable tapped density was achieved at a coprecipitation tem-

perature of 40 °C. Higher temperatures, especially 60 °C, resulted in the cracking of the secondary particles. Therefore, based on the observations made in Fig. 2, the precipitation temperature 40 °C was selected to further studies.

3.2 Effect of Coprecipitation Conditions on Particle Size Growth

During the reaction, $Ni(OH)_2$ precipitation occurred as follows:

Metal–ammonia complex formation:

$$Ni^{2+} + nNH_3 \rightarrow \left[Ni(NH_3)_n\right]^{2+} \quad (1)$$

Metal–hydroxide precipitation reaction:

$$\left[Ni(NH_3)_n\right]^{2+} + 2OH^- \rightarrow Ni(OH)_2 + nNH_3 \quad (2)$$

The formation of transition metal hydroxide precursors from a metal sulfate solution involves several physicochemical phenomena. Due to their high solubility product, transition metal sulfates readily dissolve in water. If the pH of the solution is increased by adding NaOH, transition metal hydroxides are precipitated. In the case of impure solutions, impurity phases may form [16] in the presence of transition metals and group II/III metals.

Particle size growth during $Ni(OH)_2$ coprecipitation (Fig. 4) at 40 °C was followed by determining the particle size distribution as described in Sect. 2.1. During the first stage of the precipitation process, a particle population with a homogeneous size was formed. As the population grew, the particles appeared to be dense and spherical, resulting in a narrow particle size distribution. The growth of the first particle population is presented in Fig. 4 (coprecipitation time to 22 h) and in Fig. 5 (6 h, 12 h, and 18 h). After a certain precipitation time, depending on the process conditions, a second population of small particles is formed (Fig. 3, precipitation time of 24 h; Fig. 5, 24 h). The formation of the second particle population can also be seen as a bimodal particle size distribution curve (Fig. 3).

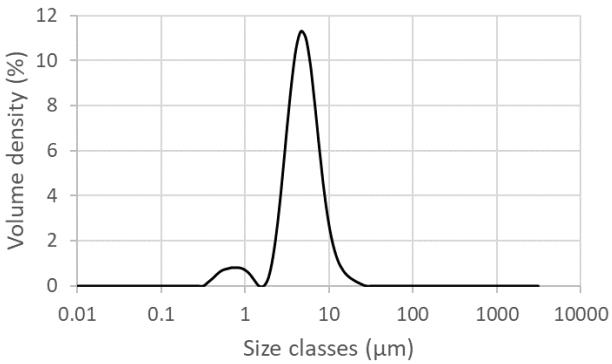

Figure 3. Bimodal particle size distribution after 30 h of precipitation (D50: 5 µm; tapped density: 2.1 g cm^{-3}).

The growth of the first population subsequently slowed down and finally ceased. Lastly, the system reached particle size distribution equilibrium. Due to the continuous nucleation and formation of primary particles, the system was composed of small and highly porous agglomerates, secondary particles at various growth stages, and dense particles that reached their maximum size, resulting in a fairly broad particle size distribution. In this continuous process, the system reached a steady state (Fig. 5, precipitation times of 30–33 h). After 33 h of precipitation, the particles were dense, with the tapped density of 2.1 g cm^{-3}.

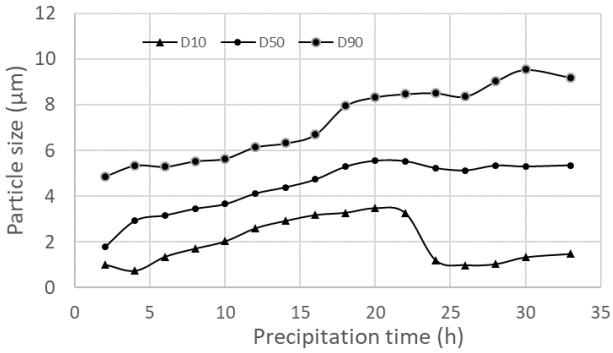

Figure 4. Evolution of $Ni(OH)_2$ particle size distribution as a function of precipitation time at 40 °C.

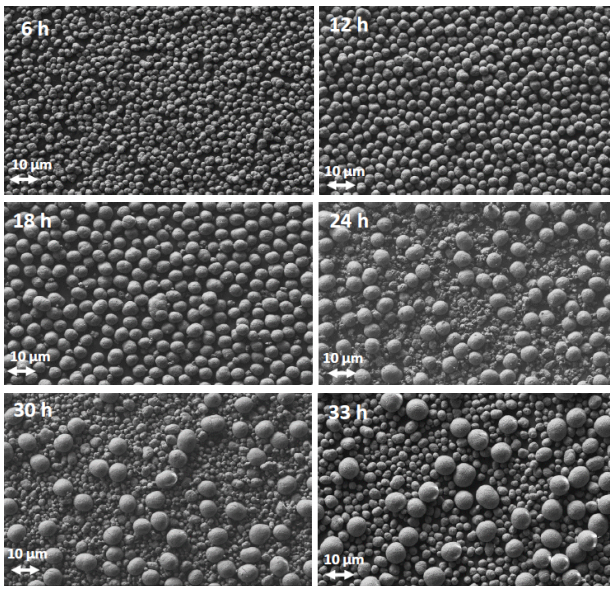

Figure 5. Evolution of particle size distribution as a function of precipitation time (6–33 h).

The growth of the first particle population and the formation of a steady-state particle size distribution in a continuous coprecipitation is presented in Fig. 5. The observed particle growth is in accordance with results reported by Zheng et al. [17].

3.3 Effect of Ammonia Concentration

As illustrated in Fig. 6, a higher ammonia concentration notably increased the growth rate of the secondary particle population. Unlike in the case of a lower ammonia concentration, the first particle population grew continuously without the spontaneous formation of a second population. Due to the higher ammonia concentration, small primary particles probably underwent dissolution/reprecipitation reactions similarly as in Ostwald ripening. The formation of the second particle population was initiated by decreasing the ammonia concentration in the mother liquor. Thus, in a CSTR precipitation process, the particle size and particle size distribution can be tailored by carefully controlling the ammonia concentration and pH level. Additionally, the residence time also affects the primary particle size growth. The shorter the residence time is, the higher is the growth rate of secondary particles. The increased growth rate may be due to a higher nucleation rate, which provides more building blocks for the growth of secondary particles. The growth of the first particle population stopped with a decreasing ammonia concentration in the mother liquor, which is in line with Barai et al. [12].

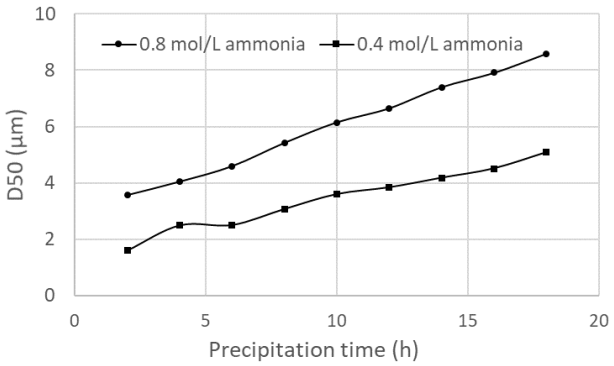

Figure 6. Effect of ammonia concentration on particle size growth rate.

3.4 Effect of Agitation Rate

Precursor properties, i.e., forming of the aggregates and the growth of the aggregates, are highly dependent on the agglomeration mechanism due to particle collisions taking place in the reactor. The fluid motion is determined by the reactor layout and the type and rate of applied agitation [18].

Homogeneous mixing is much easier to achieve in a laboratory-scale reactor than in larger-scale reactors. The linear velocity of the fluid must be greater than the settling velocity of the particles. Of course, particle size and settling velocity of the particles do not scale with the size of a reactor. High specific power input (high agitation speed) improves mixing and the homogeneity of particle suspension in the reactor. However, particle damage is an unwanted effect that is related to high agitation rates. Therefore, mixing has to be a compromise between appropriate homogeneity of the suspension (high agitation rate preferred) and avoidance of unadvantageous processes like particle damages (low agitation rate preferred).

The effect of applied agitation energy on the tap density and specific capacity has been reported by Pu et al. [19]. Increased agitation energy has a positive effect on tap density, but too vigorous agitation results in decreased specific capacity properties. Agitation is one possible parameter to control the particle growth and particle size distribution. By raising the agitation energy, the particle size can be decreased when approaching a steady state in a continuous coprecipitation process (Fig. 7).

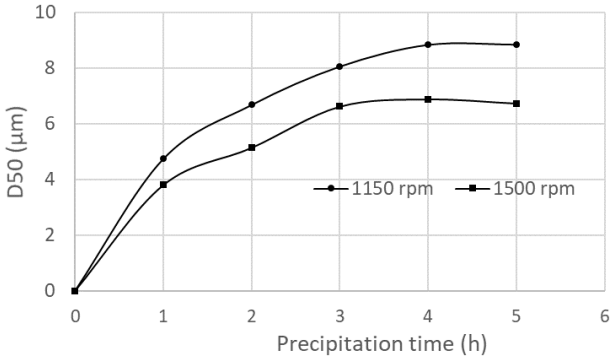

Figure 7. Effect of agitation rate on the particle size growth.

3.5 Effect of Residence Time

In a coprecipitation process, precursor particles develop from an amorphous material to dense and spherical secondary particles having a mean particle size of several micrometers. Under appropriate reaction conditions, the growth of secondary particles take place in radial direction, thus resulting in the presence of radially orientated crystallites inside the particle [20]. A radial growth of a secondary particle observed in the present study is presented in a cross-sectional SEM image in Fig. 8.

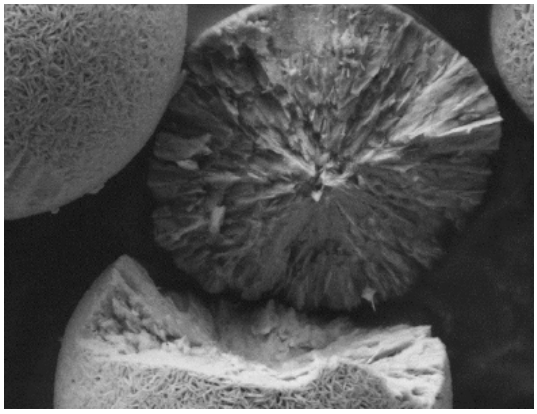

Figure 8. Radially orientated crystallites in a secondary particle.

A shorter residence time enhanced significantly the growth rate of the first particle population during the first hours of the precipitation as demonstrated in Fig. 9. The increased growth rate may be due to higher nucleation rate, thus providing more "building blocks" for the growth of secondary particles.

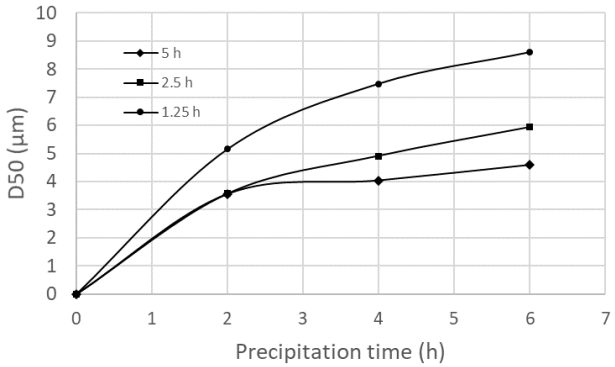

Figure 9. Effect of residence time on the growth rate of the first particle population in a continuous coprecipitation.

In a continuous coprecipitation process the residence time has a significant effect on the tap density and the morphology of precipitated secondary particles (Fig. 10).

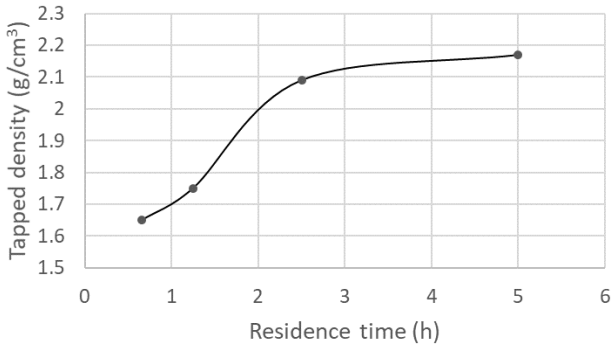

Figure 10. Effect of residence time on tap density in a continuous coprecipitation.

Under the used coprecipitation conditions, residence times that are shorter than 2.5 h resulted in unwanted properties of the product. In such cases, the average residence time in the reactor is too short for the secondary particles to achieve the desired physical properties such as spherical morphology and high tap density.

4 Conclusions

The aim of the present paper was to study the effect of reaction parameters on the coprecipitation of nickel hydroxide cathode precursor materials. In a series of coprecipitation experiments, the effect of process variables, such as reactant concentration, ammonia concentration, residence time, and agitation rate, was studied.

The main conclusions of this research are as follows:

- A homogeneous particle population with a narrow particle size distribution is always formed before a steady state. A semi-batch type coprecipitation can be applied to produce high-quality precursor particles. In a steady-state precipitation, a heterogeneous particle population was formed varying from small, porous particles to large and dense particles, thus resulting in the broadening of the particle size distribution.
- The concentration of ammonia had a significant effect on the growth rate of precursor particles. Furthermore, by adjusting the ammonia concentration of the mother liquor the formation of a new particle population can be controlled.
- The residence time has a notable impact on the physical properties of the product particles. Shortened residence times resulted in a product with smaller particle size, but also significantly decreased tap density values as well as resulted in poorer morphology of the particles. In CSTR precipitation with short residence times, a sufficient concentration of ammonia is essential in order to achieve proper tap density for the product. The size of the product particles can also be affected with an efficient agitation in the precipitation reactor.

Although knowing a well-known disadvantage of having numerous conjugated precipitation variables that affect the quality of the product, CSTR precipitation can be used for the production of precursor material with desired properties by a strict control of the precipitation conditions.

Acknowledgment

The authors acknowledge Business Finland for research funding 2021–2024 (University of Oulu, BATCircle2.0, No. 44612/31/2020). Dr. Tao Hu is acknowledged for FESEM analyses.

The authors have declared no conflict of interest.

Symbols used

D10	[µm]	10 % of particles are smaller than the given D10 value
D50	[µm]	50 % of particles are smaller than the given D50 value
D90	[µm]	90 % of particles are smaller than the given D90 value

Abbreviations

CAM	cathode active material
CSTR	continuous stirred-tank reactor
LIB	lithium-ion battery
LNO	lithium nickel oxide
pCAM	precursor for cathode active material
SEM	scanning electron microscopy

References

[1] G. E. Blomgren, *J. Electrochem. Soc.* **2017**, *164*, A5019–A5025. DOI: https://doi.org/10.1149/2.0251701jes
[2] H. Arai, S. Okada, H. Ohtsuka, M. Ichimura, J. Yamaki, *Solid State Ionics* **1995**, *80*, 261–269. DOI: https://doi.org/10.1016/0167-2738(95)00144-U
[3] T. Ohzuku, A. Ueda, M. Nagayama, *J. Electrochem. Soc.* **1993**, *140*, 1862–1870. DOI: https://doi.org/10.1149/1.2220730

[4] J. Välikangas, P. Laine, M. Hietaniemi, T. Hu, P. Tynjälä, U. Lassi, *Appl. Sci.* **2020**, *10 (24)*, 8988. DOI: https://doi.org/10.3390/app10248988

[5] J. Välikangas, P. Laine, M. Hietaniemi, T. Hu, M. Selent, P. Tynjälä, U. Lassi, *J. Solid State Electrochem.* **2023**, *27*, 641–654. DOI: https://doi.org/10.1007/s10008-022-05356-y

[6] Y.-Q Sun, W. Fu, Y.-X. Hu, J. Vaughan, L.-Z. Wang, *Tungsten* **2021**, *3*, 245–259. DOI: https://doi.org/10.1007/s42864-021-00083-9

[7] L.-W. Liang, K. Du, Z.-D. Peng, Y.-B. Cao, G.-R. Hu, *Chin. Chem. Lett.* **2014**, *25*, 883–886. DOI: https://doi.org/10.1016/j.cclet.2014.04.005

[8] F. Zhou, X. M. Zhao, A. van Bommel, A. W. Rowe, J. R. Dahn, *Chem. Mater.* **2010**, *22*, 1015–1021. DOI: https://doi.org/10.1021/cm9018309

[9] H. Liu, Y. P. Wu, E. Rahm, R. Holze, H. Q. Wu, *J. Solid State Electrochem.* **2004**, *8*, 450–466. DOI: https://doi.org/10.1007/s10008-004-0521-1

[10] X. Jiang, Y. Sha, R. Cai, Z. Shao, *J. Mater. Chem. A* **2015**, *3*, 10536–10544. DOI: https://doi.org/10.1039/C5TA01236H

[11] H. Dong, G. M. Koenig Jr., *CrystEngComm* **2019**, *22*, 1514–1530. DOI: https://doi.org/10.1039/c9ce00679f

[12] P. Barai, Z. Feng, H. Kondo, V. Srinivasan, *J. Phys. Chem. B* **2019**, *123 (15)*, 3291–3303. DOI: https://doi.org/10.1021/acs.jpcb.8b12004

[13] C.-C. Yang, *Int. J. Hydrogen Energy* **2002**, *27*, 1071–1081. DOI: https://doi.org/10.1016/S0360-3199(02)00013-7

[14] E. Weiwei, J. Cheng, C. Yang, Z. Mao, *Chin. J. Chem. Eng.* **2015**, *23*, 860–867. DOI: https://doi.org/10.1016/j.cjche.2014.04.004

[15] N. Djoudi, M. Le Page Mostefa, H. Muhr, *Chem. Eng. Technol.* **2021**, *44*, 962–971. DOI: https://doi.org/10.1002/ceat.202000330

[16] T. Kauppinen, T. Vielma, J. Salminen, U. Lassi, *ChemEngineering* **2020**, *4 (2)*, 40–56. DOI: https://doi.org/10.3390/chemengineering4020040

[17] Z. Zheng et al., *ACS Sustainable Chem. Eng.* **2018**, *6 (11)*, 13977–13982. DOI: https://doi.org/10.1021/acssuschemeng.8b02405

[18] M. Jaszczur, A. Mlynarczykowska, *Processes* **2020**, *8 (8)*, 982. DOI: https://doi.org/10.3390/pr8080982

[19] W. Pu, X. He, J. Li, J. Ying, C. Jiang, C. Wan, *J. New Mater. Electrochem. Syst.* **2005**, *8*, 235–241.

[20] M.-X. Peng, X.-Q. Shen, *J. Cent. South Univ. Technol.* **2007**, *14*, 310–314. DOI: https://doi.org/10.1007/s11771-007-0061-9

Research Article: A precursor determines the properties of cathode active material in batteries. Physical properties like particle morphology and tapped density can be controlled by optimized precipitation conditions. The effect of precipitation parameters, i.e., temperature, pH, molar ratios of reactants, agitation rate, and residence time, on the formation of dense, homogeneous, and spherical secondary particles is evaluated.

Effect of Reaction Conditions on the Coprecipitation of $Ni(OH)_2$ for Lithium-Ion Batteries

Pekka Tynjälä*, Petteri Laine, Juho Välikangas, Toni Kauppinen, Ulla Lassi

Chem. Eng. Technol. **2023**, *46 (XX)*, XXX … XXX

DOI: 10.1002/ceat.202300086